

Infrared magnetospectroscopy of graphite in tilted fields

N. A. Goncharuk,^{1,*} L. Nádorník,^{1,2} C. Faugeras,³ M. Orlita,^{2,3,†} and L. Smrčka^{1,‡}

¹*Institute of Physics, Academy of Science of the Czech Republic, v.v.i., Cukrovarnická 10, 162 53 Prague 6, Czech Republic*

²*Charles University in Prague, Faculty of Mathematics and Physics, Ke Karlovu 3, 121 16 Praha 2, Czech Republic*

³*Laboratoire National des Champs Magnétiques Intenses, CNRS-UJF-UPS-INSA, 25, avenue des Martyrs, 38042 Grenoble, France*

(Received 10 August 2012; published 8 October 2012)

The electronic structure of Bernal-stacked graphite subjected to tilted magnetic fields has been investigated using infrared magnetotransmission experiments. With the increasing in-plane component of the magnetic field B_{\parallel} , we observe significant broadening and partially also splitting of interband inter-Landau-level transitions, which originate at the H point of the graphite Brillouin zone, where the charge carriers behave as massless Dirac fermions. The observed behavior is attributed to the lifting of the twofold degeneracy of Landau levels at the H point—a degeneracy which in graphite complements the standard spin and valley degeneracies typical of graphene.

DOI: [10.1103/PhysRevB.86.155409](https://doi.org/10.1103/PhysRevB.86.155409)

PACS number(s): 71.20.-b, 71.70.Di

I. INTRODUCTION

It was the fabrication of single-layer graphene^{1,2} and subsequent discovery of massless Dirac fermions^{3,4} which triggered the present increased interest in the electrical and optical properties of graphite^{5–17}—a supposedly well-known material for condensed-matter physics.

Even though graphene is a purely two-dimensional (2D) system and graphite is characterized by a (highly anisotropic but still) clearly three-dimensional (3D) band structure, these materials, as demonstrated experimentally,^{8,10,18} share surprisingly similar optical response when the magnetic field \mathbf{B} is applied perpendicularly to the layers. A simple model, invoking inter-Landau-level (LL) excitations between highly degenerated Landau levels (LLs) of massless Dirac fermions, implies a magneto-optical response that is linear in \sqrt{B} (see, e.g., Refs. 19–26) and is capable of accounting for a significant part of the magneto-optical data acquired on graphite. Importantly, these data come not only from recent magnetotransmission studies of thin specimens^{8,10,11} but also from original measurements carried out in the late seventies,²⁷ in which \sqrt{B} -scaled spectral features have been observed using magnetoreflexion techniques. This pioneering work is a good candidate for the first direct experimental observation of massless Dirac fermions, which in bulk graphite coexist with massive particles and which provide more conventional, i.e., linear, response in B .^{28,29}

The electronic band structure of graphite in the magnetic field is mostly described using the standard model proposed by Slonczewski, Weiss, and McClure (SWM),^{30,31} even though presumably more precise but at the same time also more time-consuming approaches appeared recently (see, e.g., Refs. 32 and 33). The SWM model was derived in late fifties using mostly symmetry arguments; it describes the electronic structure near the H - K - H edge of the Brillouin zone with energies not too distant from the Fermi level. Six of the seven parameters in the SWM model, $\gamma_0, \dots, \gamma_5$,³⁴ are usually interpreted as tight-binding hopping integrals between the nearest-neighbor and partially also next-nearest-neighbor atoms. An additional parameter Δ , related to the nonequivalence of carbon atoms in A and B positions, is referred to as a pseudogap. All parameters

must be considered rather as adjustable parameters than true hopping integrals and are usually obtained by fitting either experimental data or the results of *ab initio* calculations.³⁵ The importance of individual parameters significantly varies, depending on the type of experimental data for interpretation of which the SWM model is used.

For instance, the periods of Shubnikov-de Haas^{6,36–38} (SdH) and de Haas-van Alphen^{39,40} (dHvA) oscillations depend on the extremal cross sections of the complex Fermi surface and all SWM tight-binding parameters must be properly taken into account. Similarly, cyclotron resonance experiments,^{28,41,42} which are also sensitive to the immediate vicinity of the Fermi level and which provide fairly rich response, can be hardly understood without the full SWM model.

On the other hand, interband transitions between electronic states far away from the Fermi surface can be successfully described using a simplified approach,^{10,11} which models the magneto-optical response of bulk graphite as a sum of responses of an effective graphene bilayer and of a monolayer.⁴⁴ Notably, the physical properties of a 3D system are thus described using responses of two purely 2D materials, and interestingly, not more than two coupling constants, intralayer γ_0 and interlayer γ_1 , are needed in the very first approach.⁴⁵ Within such a minimal model, the H point provides a response similar to that of a single graphene sheet, but richer due to an additional twofold degeneracy. The K point behaves as bilayer graphene, however, with an interlayer coupling twice enhanced as compared to that of the true bilayer. Limits of this model have been found, e.g., by revealing the electron-hole asymmetry at the K point of bulk graphite in recent magnetotransmission,¹¹ magnetoreflexion,^{14,17} and magneto-Raman studies.^{15,16} The full SWM model has to be used in such a case to get a quantitative agreement between experimental data and theory.

In this paper, we set other limitations of the effective monolayer and bilayer model for the magneto-optical response of graphite. Namely, we test its applicability in experiments performed in the tilted-field configuration, $\mathbf{B} = (0, B_{\parallel}, B_{\perp})$, which is a basic tool to distinguish between 2D and 3D character of condensed-matter systems. We focus on the graphenelike

signal from the H point and show that the magneto-optical response of graphite in a tilted magnetic field follows the total magnetic field and not only its perpendicular component, as should be in the case of an ideal 2D system. The infrared magnetotransmission technique is thus, perhaps surprisingly, significantly more sensitive to the in-plane component of the magnetic field as compared to other techniques such as SdH or dHvA oscillations, which reveal the 3D character of graphite only for rather high tilting angles.^{38,40} To interpret our data, we use the recently developed theory of the graphite band structure subject to a tilted magnetic field, which predicts the lifting of the twofold degeneracy at the H point.⁴³ This degeneracy, taking origin in the 3D character of graphite (four atoms in a unit cell instead of two for graphene), is an additional one to the valley and spin degeneracies in graphene.

II. EXPERIMENT

Thin graphite specimens for our magnetotransmission study have been prepared by exfoliation. A thin layer of bulk graphite, with an average thickness around ≈ 100 nm, was located on the scotch tape used for exfoliation. This tape has several relatively wide spectral windows with a sufficiently high optical transmission. A high-quality natural graphite crystal has been chosen for exfoliation, since it provides equivalent but better pronounced magneto-optical response as compared to, e.g., highly oriented pyrolytic graphite.⁹ The

magnetotransmission spectra were measured for the magnetic field inclined with respect to the c axis of graphite by selected angles of φ , i.e., in the perpendicular ($\varphi = 0^\circ$) and several tilted-field configurations.

To measure the transmission spectra in the spectral range 100–800 meV, the nonpolarized radiation of a globar was analyzed by a Fourier transform spectrometer and guided to the sample by light-pipe optics. The sample was placed in a cryostat at a temperature of 2 K, located inside superconducting or resistive coils, which reach magnetic fields up to 13 and 28 T, respectively. The transmitted signal was detected by a composite Si bolometer. All spectra presented in this study have been normalized by the zero-field transmission.

III. RESULTS

The magnetotransmission spectra measured at three different angles between the c axis of graphite and the magnetic field, $\varphi = 0, 15,$ and 30° , are presented in Figs. 1(a)–1(c), respectively. To facilitate the identification of individual absorption lines, the transmission curves are depicted as functions of the photon energy normalized by the factor of $\sqrt{B_\perp}$, which is typical of LLs in a system of ideal 2D massless Dirac fermions. Plotted this way, we can identify graphenelike signals originating from the H point and easily follow its deviation from the $\sqrt{B_\perp}$ dependence induced by the in-plane component of the magnetic field B_\parallel . An additional set of data is presented in Fig. 2, where the magnetotransmission spectra

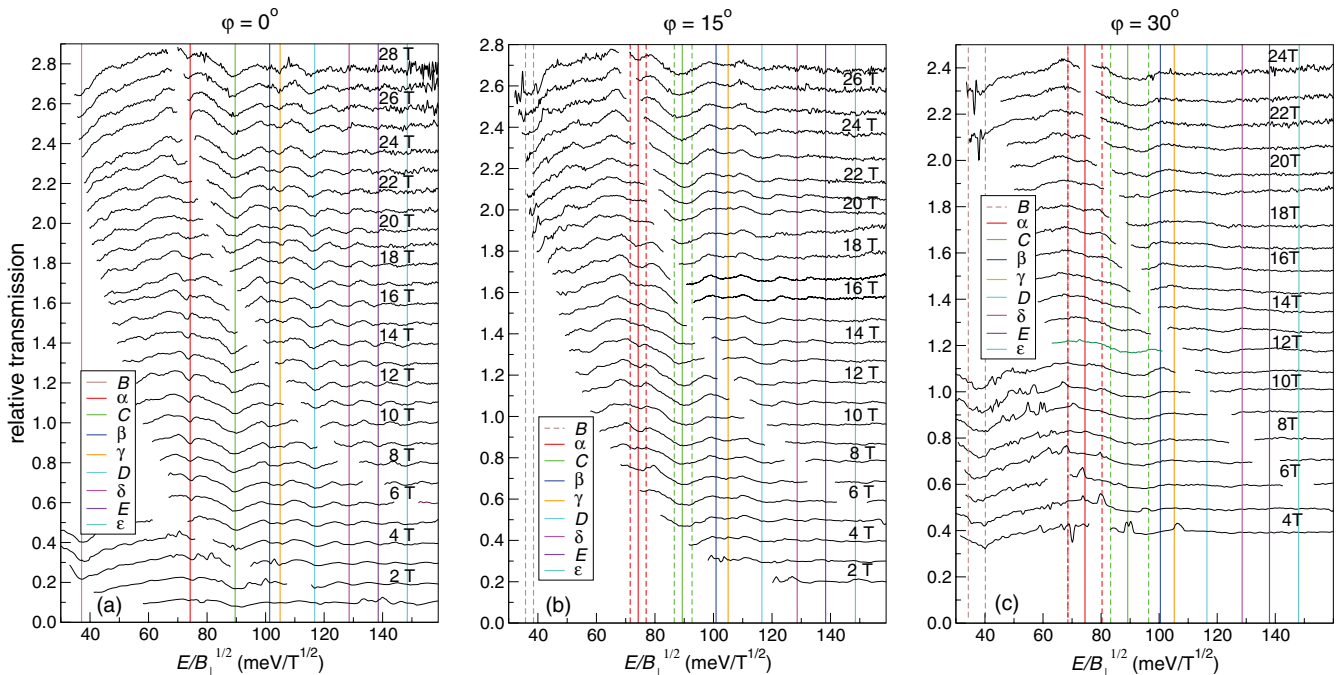


FIG. 1. (Color online) Transmission of a thin graphite specimen measured at magnetic field tilted by $\varphi = 0, 15,$ and 30° with respect to the c axis of graphite. Values nearby individual curves always denote the component of the magnetic field perpendicular to the graphite layer B_\perp . The missing parts of spectra correspond to regions in which the supporting tape is completely opaque. The energy axis for each curve is rescaled by a factor of $\sqrt{B_\perp}$ to facilitate identification of spectral features originating at the H point of graphite. Vertical lines correspond to positions of van Hove singularities in the joint density of states as calculated using the minimal nearest-neighbor tight-binding model.⁴³ Since the lifting of degeneracy exactly at the H point is governed by the coupling constants $T_{n,n+1} \propto \sqrt{B_\perp} \tan(\varphi)$, the positions of these van Hove singularities remain constant in these figures. For clarity, successive spectra in (a)–(c) are shifted vertically by 0.1.

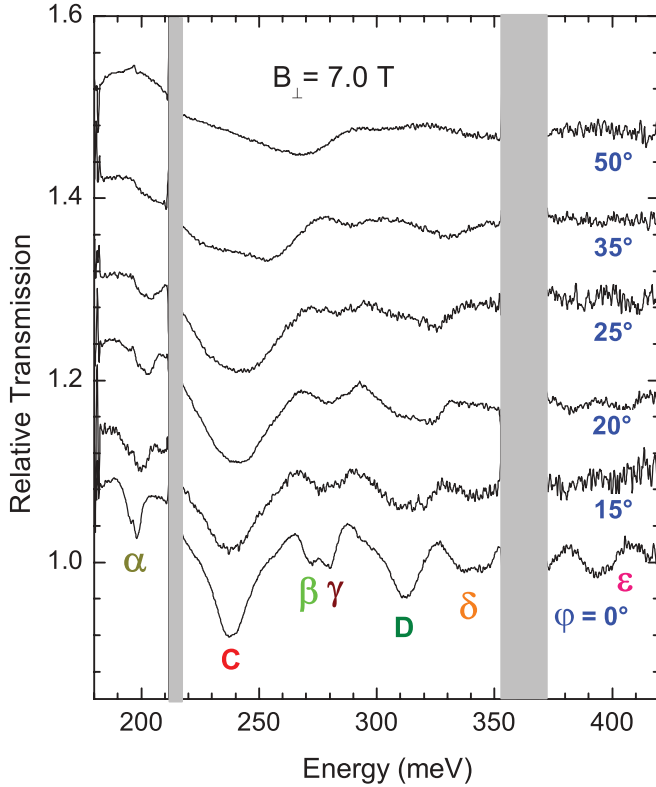


FIG. 2. (Color online) Relative magnetotransmission spectra for tilting angles $\varphi = 0, 15, 20, 25, 35$, and 50° taken with the same perpendicular component of the field $B_\perp = 7$ T. The broadening of the lines with increasing angle, i.e., with the increasing in-plane component of the field B_\parallel , is well visible, e.g., on the C line, the width of which increases roughly linearly with B_\parallel . A sample different from Fig. 1 has been used (with higher density of crystallites and their average thickness). For clarity, successive spectra are shifted vertically by 0.1.

for several tilting angles φ are presented, all measured at a fixed perpendicular component of the field $B_\perp = 7$ T.

The observed absorption lines have been marked consistently with the notation introduced earlier.^{8,19} The transitions denoted by Roman letters have their direct counterpart in the response of graphene,¹⁹ while the “Greek” lines are characteristic of graphite.⁸ They are, in principle, dipole-forbidden in a pure 2D system of Dirac fermions, nevertheless they can be consistently explained with the standard dipole selection rule ($n \rightarrow n \pm 1$) when the twofold degeneracy of LLs at the H points of bulk graphite is properly considered. Let us note that the widths of absorption lines not only reflect the naturally present disorder in the graphite crystal but they are also partially given by the profile of the individual Landau sub-bands in the vicinity of the H point.¹⁸

The transmission spectra measured at $\varphi = 0^\circ$, presented in Fig. 1(a), are fully analogous to previous experiments^{8,10,11} and the color vertical lines mark transmission minima proportional to $\sqrt{B_\perp}$. All such transitions originate from the H point. The transmission minima are more pronounced at lower energies and their width increases with increasing magnetic field. Interestingly, the number of observed transitions remains nearly constant with B_\perp . This behavior reflects the specific

energy dependence of the relaxation rate (i.e., broadening of lines), $\tau^{-1}(E) \propto |E|$, which maps the (linear in energy) density of states around the H point. An analogous effect has been recently observed also in graphene specimens.⁴⁶

For a nonzero tilting angle φ , the observed magnetotransmission spectra significantly deviate from expectations for a purely 2D system, which is, in the case of orbital effects, only sensitive to the perpendicular component of the field. At φ as low as 15° [see Fig. 1(b)], the transitions denoted by Roman letters change shapes and broaden, while the Greek lines become significantly weaker. For $\varphi > 30^\circ$, the Greek lines completely disappear from the spectra and the Roman lines are also much less pronounced as a result of a significant broadening. Alternatively, we can follow these effects in Fig. 2, where the magnetotransmission spectra are plotted at several angles with the perpendicular component of the field kept constant, $B_\perp = 7$ T. The effects induced by the in-plane component of the field B_\parallel are well illustrated, e.g., on the C line. With increasing tilt angle, this line not only significantly broadens but also gains a complex structure—a strong asymmetry is developed and the line becomes nearly split into two components for higher angles ($\varphi > 25^\circ$).

IV. DISCUSSION

To interpret the broadening of absorption lines with B_\parallel , we will consider the electronic band structure at the H point of graphite in detail. In particular, we will focus on the B_\parallel -induced lifting of the twofold degeneracy, which in graphite complements the spin and valley degeneracies in graphene, and follow the theory recently developed by Goncharuk and Smrčka.⁴³ The additional twofold degeneracy may be interpreted as a direct consequence of the effectively vanishing interlayer interaction for a charge carrier with the momentum $k_z d = \pi/2$, where d is the interlayer distance. The reason is that the neighboring graphene sheets are rotated by 30° . If the field dependence of the energy in even layers is $E_n^e \propto \pm \sqrt{B_\perp n}$ then the energy in odd layers reads $E_n^o \propto \pm \sqrt{B_\perp (n+1)}$, where $n = 0, 1, \dots$ is the index of the LLs. Two states $|n+1\rangle^e$ and $|n\rangle^o$ belonging to degenerated eigenenergies $E_{n+1}^e = E_n^o$ are orthogonal and, therefore, the corresponding interlayer hopping integral is equal to zero for $B_\parallel = 0$. In tilted configuration, the in-plane field component B_\parallel shifts the mutual position of centers of orbits $|n+1\rangle^e$ and $|n\rangle^o$ in real space by $y_0 = d B_\parallel / B_\perp$. The orbits are no longer exactly orthogonal and the interlayer interaction does not completely vanish. In the lowest order of the perturbation theory we get instead of E_n^o and E_{n+1}^e four energies $E_{n,n+1}^{o,e'} = \pm T_{n,n+1} \pm [(E_n^o)^2 + T_{n,n+1}^2]^{1/2}$ where $T_{n,n+1} = \gamma_1 d \tan(\varphi) \sqrt{B_\perp |e|(n+1)/(2\hbar)}$.⁴³ Let us note that another theory presented in Ref. 47 is devoted to the case of magnetic field applied strictly parallel to the sheets of the graphene bilayer and multilayers including graphite. It is suggested that the obtained energy spectrum can be verified experimentally using electron tunneling or optical spectroscopy.

Obviously, the first-order perturbation theory employed in Ref. 43, which involves only two states with the same energy exactly at $k_z d = \pi/2$, is not the best approximation and overestimates the splitting. It is acceptable only for rather small tilting angles and LLs with limited n . For this reason, we have

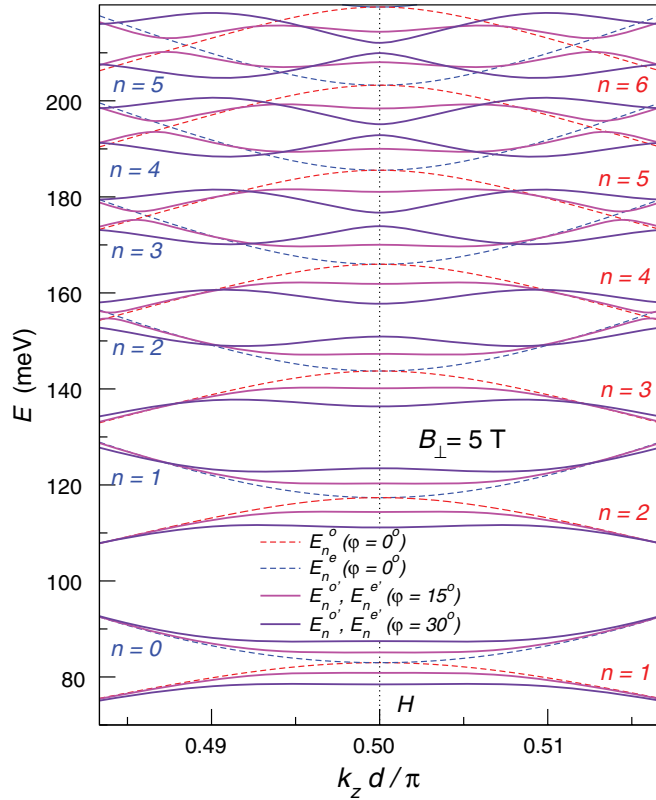


FIG. 3. (Color online) Landau sub-bands in the vicinity of the H points, $k_z d = \pi/2$, at $B_{\perp} = 5$ T. The solid and dashed lines describe the k_z dependence of energies E_n^e and E_n^o in even and odd graphene sheets at $\varphi = 0, 15$, and 30° .

calculated the eigenenergies numerically employing a larger basis, which allows us to calculate also the k_z dependence in the vicinity of the H points. The results are shown in Fig. 3. Dashed lines describe the k_z dependence of energies E_n^e and E_n^o in even and odd graphene sheets at $\varphi = 0^\circ$. Solid lines describe the energies E_n^e and E_n^o , both at $\varphi = 15$ and 30° , resolved by different colors. The corresponding eigenstates mix the wave functions from both even and odd layers, nevertheless the same notation is kept to emphasize to what energies E_n^e and E_n^o are reduced for $\varphi \rightarrow 0$.

Our numerical calculations reveal the importance of the states in the vicinity of the H point. Two side extrema in the k_z dependence of energy sub-bands appear and the curvature of the k_z curves is reversed at the H point. Each new local extremum developed along the k_z dependence of the energy sub-bands adds a new van Hove singularity to the (joint) density of states. The energy gap opened between sub-bands appears slightly away from the H point and it decreases with the increasing LL index n ($n \geq 2$). Unlike the splitting directly at the H point, this energy gap is no longer proportional to $\sqrt{B_{\perp}}$.

At $\varphi = 0$, each absorption line consists of up to four degenerate transitions. To be more specific, we have two transitions for each Greek line and also for the B line; the rest of the lines denoted by Roman letters include four degenerate transitions, with four corresponding (degenerate) van Hove singularities in the joint density of states (for details see

Refs. 8 and 18). At $\varphi = 0$, positions of these singularities are represented in Fig. 1(a) by the vertical color lines. The situation becomes more complex at $\varphi > 0$, when the degeneracy of these four Van Hove singularities is lifted. In addition, other singularities, presumably weaker, develop in the vicinity of the H point. To illustrate the strength of the effects induced by the in-plane magnetic field, we plot in Figs. 1(b) and 1(c) the positions of four main singularities in the limits of validity of the first-order approximation—those which originate directly from the H point. Two of them remain almost degenerate. On the other hand, for the sake of clarity, we do not mark positions of additional singularities developed due to anticrossing of Landau sub-bands further from the H point. To justify this, we note that such singularities in principle exist even at $B_{\parallel} = 0$ due to the trigonal warping term γ_3 ,⁴⁸ which is neglected in the simple effective monolayer and bilayer model. Nevertheless, they have not been observed in the experiment in perpendicular fields.⁸

To sum up, the in-plane magnetic field profoundly modifies the profile of Landau sub-bands at the H point of bulk graphite. A series of minigaps is created already within the first order of the perturbation theory, which is directly reflected by the newly developed van Hove singularities in the joint density of states. Experimentally, this leads to a splitting of the observed dipole-allowed transitions with the increasing angle φ , or at least, if disorder effects are realistically involved, to a significant broadening of these transitions. This splitting and broadening increases, at a fixed B_{\perp} , roughly linearly with B_{\parallel} , or equivalently, approximately scales as $\sqrt{B_{\perp}}$ when the tilting angle φ is kept constant. Such behavior is consistent with the experimental data plotted in Figs. 2 and 1(a)–1(c), respectively.

V. CONCLUSIONS

The electronic band structure at the H point of bulk graphite has been studied using the infrared transmission technique in magnetic fields tilted with respect to the c axis of this material. While for the magnetic field applied along this axis the magneto-optical responses of graphite (due to the H point) and graphene (due to the K point) closely resemble each other, pronounced deviations clearly appear with increasing tilt angles. The 3D nature of the electronic band structure of bulk graphite is thus revealed at significantly lower tilting angles as compared to SdH and dHvA measurements.^{38,40}

In addition, our results show another difference in the properties of graphite and of multilayer epitaxial graphene, both of which are materials composed of layered graphene sheets and the nature of which is still subject to live discussions. While the response of Bernal-stacked graphite is, as demonstrated in this work, profoundly modified by the in-plane component of the magnetic field, no such effects have been observed for multilayer epitaxial graphene,¹⁹ in which the unique rotational stacking of adjacent layers⁴⁹ ensures its dominantly 2D character. In a very good approximation, the multilayer epitaxial graphene thus may be considered as a material consisting of a number of mutually independent (uncoupled) graphene layers.

ACKNOWLEDGMENTS

We thank M. Potemski for valuable discussions. The support of the following projects is acknowledged: European Science Foundation Epitaxial Graphene Transistor (EPIGRAT) Project GRA/10/E006; Grant Agency of the Czech Republic Grant No. P204/10/1020 “Magneto-spectroscopy of

Dirac fermions”; programme “Transnational access” Contract No. 228043-EuroMagNET II-Integrated Activities; Academy of Sciences of the Czech Republic research programmes AVOZ10100521 and “Nanotechnology for Society” (project KAN400100652); and Charles University in Prague Grant GAUK No. SVV-2012-265306.

*Present address: ABB s.r.o., Semiconductors, R&D, Novodvorská 1768/138a, 14221 Prague, Czech Republic.

†orlita@karlov.mff.cuni.cz

‡smrcka@fzu.cz

¹C. Berger, Z. Song, T. Li, X. Li, A. Y. Ogbazghi, R. Feng, Z. Dai, A. N. Marchenkov, E. H. Conrad, P. N. First, and W. A. de Heer, *J. Phys. Chem. B* **108**, 19912 (2004).

²K. S. Novoselov, A. K. Geim, S. Morozov, D. Jiang, M. I. Katsnelson, I. Grigorieva, S. Dubonos, and A. A. Firsov, *Science* **306**, 666 (2004).

³K. S. Novoselov, A. K. Geim, S. V. Morozov, D. Jiang, M. I. Katsnelson, I. V. Grigorieva, S. V. Dubonos, and A. A. Firsov, *Nature (London)* **438**, 197 (2005).

⁴Y. Zhang, Y.-W. Tan, H. L. Stormer, and P. Kim, *Nature (London)* **438**, 201 (2005).

⁵Z. Q. Li, S.-W. Tsai, W. J. Padilla, S. V. Dordevic, K. S. Burch, Y. J. Wang, and D. N. Basov, *Phys. Rev. B* **74**, 195404 (2006).

⁶I. A. Luk'yanchuk and Y. Kopelevich, *Phys. Rev. Lett.* **97**, 256801 (2006).

⁷J. C. González, M. Muñoz, N. García, J. Barzola-Quiquia, D. Spoddig, K. Schindler, and P. Esquinazi, *Phys. Rev. Lett.* **99**, 216601 (2007).

⁸M. Orlita, C. Faugeras, G. Martinez, D. K. Maude, M. L. Sadowski, and M. Potemski, *Phys. Rev. Lett.* **100**, 136403 (2008).

⁹M. Orlita, C. Faugeras, G. Martinez, D. K. Maude, M. L. Sadowski, J. M. Schneider, and M. Potemski, *J. Phys.: Condens. Matter* **20**, 454223 (2008).

¹⁰M. Orlita, C. Faugeras, J. M. Schneider, G. Martinez, D. K. Maude, and M. Potemski, *Phys. Rev. Lett.* **102**, 166401 (2009).

¹¹K.-C. Chuang, A. M. R. Baker, and R. J. Nicholas, *Phys. Rev. B* **80**, 161410 (2009).

¹²Z. Zhu, H. Yang, B. Fauqué, Y. Kopelevich, and K. Behnia, *Nat. Phys.* **6**, 26 (2010).

¹³N. Ubrig, P. Plochocka, P. Kossacki, M. Orlita, D. K. Maude, O. Portugall, and G. L. J. A. Rikken, *Phys. Rev. B* **83**, 073401 (2011).

¹⁴L. C. Tung, P. Cadden-Zimansky, J. Qi, Z. Jiang, and D. Smirnov, *Phys. Rev. B* **84**, 153405 (2011).

¹⁵P. Kossacki, C. Faugeras, M. Kühne, M. Orlita, A. A. L. Nicolet, J. M. Schneider, D. M. Basko, Y. I. Latyshev, and M. Potemski, *Phys. Rev. B* **84**, 235138 (2011).

¹⁶Y. Kim, Y. Ma, A. Imambekov, N. G. Kalugin, A. Lombardo, A. C. Ferrari, J. Kono, and D. Smirnov, *Phys. Rev. B* **85**, 121403 (2012).

¹⁷J. Levallois, M. Tran, and A. B. Kuzmenko, *Solid State Commun.* **152**, 1294 (2012).

¹⁸M. Orlita, C. Faugeras, G. Martinez, D. K. Maude, J. M. Schneider, M. Sprinkle, C. Berger, W. A. de Heer, and M. Potemski, *Solid State Commun.* **149**, 1128 (2009).

¹⁹M. L. Sadowski, G. Martinez, M. Potemski, C. Berger, and W. A. de Heer, *Phys. Rev. Lett.* **97**, 266405 (2006).

²⁰V. P. Gusynin, S. G. Sharapov, and J. P. Carbotte, *Phys. Rev. Lett.* **98**, 157402 (2007).

²¹Z. Jiang, E. A. Henriksen, L. C. Tung, Y.-J. Wang, M. E. Schwartz, M. Y. Han, P. Kim, and H. L. Stormer, *Phys. Rev. Lett.* **98**, 197403 (2007).

²²R. S. Deacon, K.-C. Chuang, R. J. Nicholas, K. S. Novoselov, and A. K. Geim, *Phys. Rev. B* **76**, 081406(R) (2007).

²³M. Orlita, C. Faugeras, P. Plochocka, P. Neugebauer, G. Martinez, D. K. Maude, A.-L. Barra, M. Sprinkle, C. Berger, W. A. de Heer, and M. Potemski, *Phys. Rev. Lett.* **101**, 267601 (2008).

²⁴I. Crassee, J. Levallois, A. L. Walter, M. Ostler, A. Bostwick, E. Rotenberg, T. Seyller, D. van der Marel, and A. B. Kuzmenko, *Nat. Phys.* **7**, 48 (2011).

²⁵I. Crassee, J. Levallois, D. van der Marel, A. L. Walter, Th. Seyller, and A. B. Kuzmenko, *Phys. Rev. B* **84**, 035103 (2011).

²⁶L. G. Booshehri, C. H. Mielke, D. G. Rickel, S. A. Crooker, Q. Zhang, L. Ren, E. H. Házoz, A. Rustagi, C. J. Stanton, Z. Jin, Z. Sun, Z. Yan, J. M. Tour, and J. Kono, *Phys. Rev. B* **85**, 205407 (2012).

²⁷T. W. W. Toy, M. S. Dressehaus, and G. Dresselhaus, *Phys. Rev. B* **15**, 4077 (1977).

²⁸J. K. Galt, W. A. Yager, and H. W. Dail, *Phys. Rev.* **103**, 1586 (1956).

²⁹P. R. Schroeder, M. S. Dresselhaus, and A. Javan, *Phys. Rev. Lett.* **20**, 1292 (1969).

³⁰J. C. Slonczewski and P. R. Weiss, *Phys. Rev.* **109**, 272 (1958).

³¹J. W. McClure, *Phys. Rev.* **119**, 606 (1960).

³²Y.-H. Ho, Y.-H. Chiu, W.-P. Su, and M.-F. Lin, *Appl. Phys. Lett.* **99**, 011914 (2011).

³³Y. H. Ho, J. Wang, Y. H. Chiu, M. F. Lin, and W. P. Su, *Phys. Rev. B* **83**, 121201 (2011).

³⁴N. B. Brandt, S. M. Chudinov, and Y. G. Ponomarev, *Semimetals I: Graphite and its Compounds*, Modern Problems in Condensed Matter Sciences, Vol. 20.1 (North-Holland, Amsterdam, 1988).

³⁵A. Grüneis, C. Attacalite, L. Wirtz, H. Shiozawa, R. Saito, T. Pichler, and A. Rubio, *Phys. Rev. B* **78**, 205425 (2008).

³⁶J. A. Woollam, *Phys. Rev. Lett.* **25**, 810 (1970).

³⁷I. A. Luk'yanchuk and Y. Kopelevich, *Phys. Rev. Lett.* **93**, 166402 (2004).

³⁸J. M. Schneider, N. A. Goncharuk, P. Vašek, P. Svoboda, Z. Vyborný, L. Smrčka, M. Orlita, M. Potemski, and D. K. Maude, *Phys. Rev. B* **81**, 195204 (2010).

³⁹S. J. Williamson, S. Foner, and M. S. Dresselhaus, *Phys. Rev.* **140**, A1429 (1965).

⁴⁰J. M. Schneider, B. A. Piot, I. Sheikin, and D. K. Maude, *Phys. Rev. Lett.* **108**, 117401 (2012).

- ⁴¹R. E. Doezema, W. R. Datars, H. Schaber, and A. Van Schyndel, *Phys. Rev. B* **19**, 4224 (1979).
- ⁴²M. Orlita, P. Neugebauer, C. Faugeras, A.-L. Barra, M. Potemski, F. M. D. Pellegrino, and D. M. Basko, *Phys. Rev. Lett.* **108**, 017602 (2012).
- ⁴³N. A. Goncharuk and L. Smrčka, *J. Phys.: Condens. Matter* **24**, 185503 (2012).
- ⁴⁴M. Koshino and T. Ando, *Phys. Rev. B* **77**, 115313 (2008).
- ⁴⁵B. Partoens and F. M. Peeters, *Phys. Rev. B* **75**, 193402 (2007).
- ⁴⁶M. Orlita, C. Faugeras, R. Grill, A. Wymolek, W. Strupinski, C. Berger, W. A. de Heer, G. Martinez, and M. Potemski, *Phys. Rev. Lett.* **107**, 216603 (2011).
- ⁴⁷S. S. Pershoguba and V. M. Yakovenko, *Phys. Rev. B* **82**, 205408 (2010).
- ⁴⁸K. Nakao, *J. Phys. Soc. Jpn.* **40**, 761 (1976).
- ⁴⁹J. Hass, F. Varchon, J. E. Millán-Otoya, M. Sprinkle, N. Sharma, W. A. de Heer, C. Berger, P. N. First, L. Magaud, and E. H. Conrad, *Phys. Rev. Lett.* **100**, 125504 (2008).